REPORT DOCUMENTATION PAGE

Form Approved
OMB No. 0704-0188

1. AGENCY USE ONLY (Leave blank)	2. REPORT DATE	3. REPORT TYPE AND DATES COVERED
	15 December 1997	Final Technical 10.1.93-9.30.97

4. TITLE AND SUBTITLE

Matter-Wave Interferometry with Laser Cooled Atoms

5. FUNDING NUMBERS

G: N00014-91-J-1198

6. AUTHOR(S)

David H. McIntyre

7. PERFORMING ORGANIZATION NAME(S) AND ADDRESS(ES)

Oregon State University
Department of Physics
Weniger Hall 301
Corvallis, OR 97331-6507

8. PERFORMING ORGANIZATION REPORT NUMBER

N0006A

9. SPONSORING/MONITORING AGENCY NAME(S) AND ADDRESS(ES)

Office of Naval Research; Dr. Herschel S. Pilloff
ONR Code 331
800 N. Quincy St.
Arlington, VA 22217-5660

10. SPONSORING/MONITORING AGENCY REPORT NUMBER

11. SUPPLEMENTARY NOTES

12a. DISTRIBUTION/AVAILABILITY STATEMENT

Public availability

12b. DISTRIBUTION CODE

13. ABSTRACT *(Maximum 200 words)*

We have developed a cold atomic beam source to be used as the input beam for a three-grating atom interferometer. Using laser cooling and trapping techniques, we have slowed and cooled a thermal atomic beam, trapped the slow atoms, and redirected them into a cold beam with an adjustable velocity. The cold atomic beam has a temperature of approximately 500 μK and has a controllable velocity from 2-20 m/s. The gratings for the interferometer have been microfabricated in silicon nitride and have a grating spacing of 250 nm.

14. SUBJECT TERMS

atom interferometry, laser cooling, laser trapping
nanofabrication, diode laser frequency stabilization

15. NUMBER OF PAGES

20

16. PRICE CODE

17. SECURITY CLASSIFICATION OF REPORT	18. SECURITY CLASSIFICATION OF THIS PAGE	19. SECURITY CLASSIFICATION OF ABSTRACT	20. LIMITATION OF ABSTRACT
unclassified	unclassified	unclassified	UL

R&T 3108128---08

MATTER-WAVE INTERFEROMETRY WITH LASER COOLED ATOMS

David McIntyre

Department of Physics, Oregon State University, Corvallis, OR 97331-6507

Grant No: N00014-91-J-1198

PR No: 97PR01050

Final Technical Report, December 1997

I. Introduction

This research program is concerned with matter-wave interferometry of laser cooled atoms. A slow beam of laser cooled rubidium atoms will be used as the matter-wave source. The atom optical elements are microfabricated amplitude transmission gratings which will be used in a three-grating interferometer to split and recombine the rubidium beam. The atomic interferometer will be a useful new tool with which to perform precision experiments in atomic physics, quantum optics, and gravitation.

The research program takes advantage of three new technologies, the combination of which provides a unique opportunity to construct a compact and stable interferometer. The techniques of laser cooling and trapping are used to produce cold rubidium atoms in a well collimated beam. Commercially available diode lasers with optical feedback frequency stabilization are used for the laser cooling and trapping beams and for atomic beam diagnostics. Finally, submicron transmission gratings made with high-resolution electron-beam lithography are used as the coherent beam splitters of the atomic interferometer.

Figure 1 shows the proposed interferometer geometry with the two paths that are generally used in such a device. The three-grating Bonse-Hart interferometer is a particularly useful design since it has intrinsically equal path lengths and is relatively insensitive to misalignments.[1,2] This same interferometer geometry was used by the MIT group in their recent work on a sodium atom

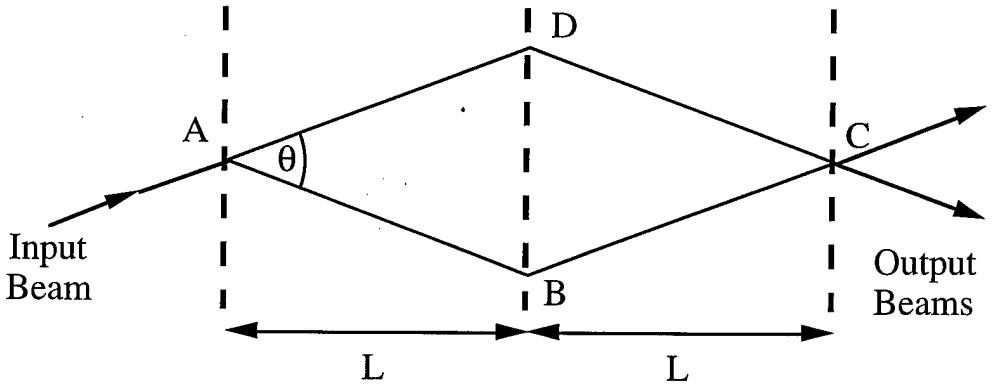

Fig. 1. Three-grating Bonse-Hart interferometer with two-path interference configuration shown.

interferometer using a supersonic beam.[3] Slow atoms have longer de Broglie wavelengths and hence allow for a more compact interferometer. Hence, as input to the interferometer, we desire a well-collimated, intense, low-velocity atomic beam. Laser cooling and trapping techniques are well suited to providing such a beam of atoms. Magneto-optic trapping is particularly appropriate since it permits spatial and velocity compression of atoms in appropriately designed magnetic and laser fields.[4] To produce a low-velocity atomic rubidium beam, we have used a two-dimensional magneto-optic trap or atomic funnel.[5] An atomic funnel for sodium was first demonstrated by Riis *et al.*[6] Related work has been reported by Nellessen *et al.*[7] with sodium and by Yu *et al.*[8] with cesium.

We have planned for a mean atomic velocity of 10 m/s, corresponding to a de Broglie wavelength of 0.5 nm. The emerging atomic beam will have a temperature of approximately 500 μK, corresponding to a coherence length of 50 wavelengths. The beam will then enter the three-grating interferometer. The amplitude transmission gratings have a period of 250 nm and are made from free-standing silicon nitride films on silicon substrates.[9] The three gratings will be separated by 5 cm and will diffract the rubidium beam by 2 mrad into the first order. Compared to the other interferometers which have been demonstrated using material structures,[3] ours is relatively compact. The ability to tune the velocity of the funnel output beam also provides our experiment with another degree of flexibility.

II. Diode laser frequency stabilization

Our original diode-laser systems used optical-feedback stabilization from Fabry-Perot confocal cavities.[10,11] We have since redirected our efforts to building and using diode-laser systems that use diffraction gratings as the feedback element.[12] These lasers are simpler to implement and have comparable performance. Figure 2 shows a schematic of the laser system. A holographic grating at the Littrow angle provides the optical feedback. The laser diode, collimator lens, and grating are all mounted on a small aluminum block for mechanical and thermal stability. Residual mechanical vibrations of the extended cavity are reduced with a servo-control system that uses the diode-laser injection current to control the laser frequency. The electronic servo-control loop has a unity-gain frequency (≈ 100 kHz) far above any mechanical resonances, so is very effective at reducing the mechanical noise in the system. To characterize the linewidth of these laser systems we have performed heterodyne measurements between a grating-feedback laser and a narrow linewidth (≈ 10 kHz) cavity-feedback laser.[10,11] We find the grating-feedback laser to have a FWHM linewidth of 150 kHz.

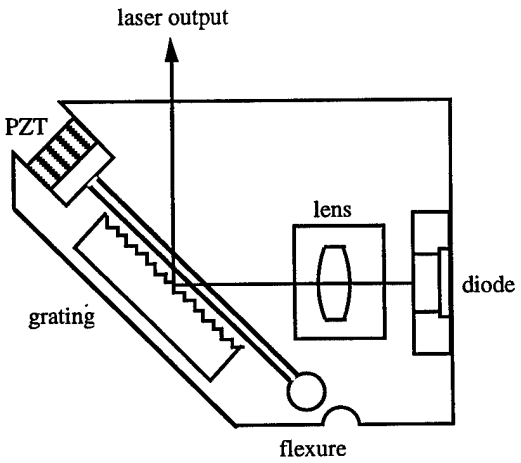

Fig. 2. Diagram of laser system with optical feedback from a diffraction grating. The grating is held with a commercial mirror mount which is not shown. The piezoelectric transducer (PZT) bends the flexure to tilt and translate the grating.

The needs of our experiment have lead us to use three different schemes to determine the diode laser frequencies. In some cases we use a confocal Fabry-Perot etalon as the frequency discriminator. The laser can then be scanned while it is locked to the etalon if the etalon length and the grating angle are synchronously ramped. The laser frequency used in a magneto-optic trap wants to be stabilized one to several linewidths (≈ 5 - 20 MHz) below the trapping transition. We have found polarization spectroscopy to be useful in these situations as it provides a dispersive signal that is optimal for locking.[13] By adjusting the electronic offset in the servo-control circuit, the laser frequency can be locked over a range of approximately 60 MHz (≈ +10 to -50 MHz). To produce the frequency shifted laser beams required in the atomic funnel, we have developed a simple electronic frequency discriminator that can be used to frequency-offset lock two lasers. The complete frequency-offset locking system is shown in Fig. 3. The frequency discriminator consists primarily of a fast comparator to convert the sinusoidal beat note into a digital signal, and a

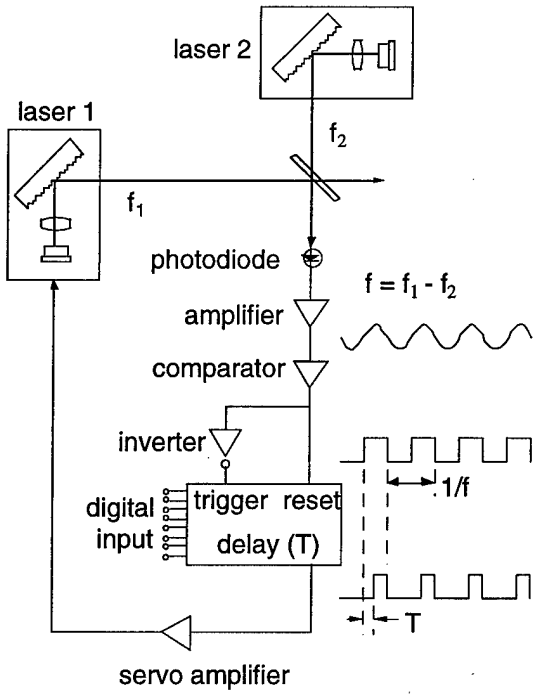

Fig. 3. Schematic of frequency-offset locking system. Not shown is the system used to stabilize laser 2 to a confocal etalon or a rubidium resonance.

digitally controllable delay generator with delay T. The delay generator output has a duty cycle of $1/2 - fT$, where f is the frequency of the beat note. A low pass filter produces a signal proportional to the duty cycle, which thus allows linear frequency discrimination from near dc to $f = 1/2T$. Using this system, we have been able to continuously tune the offset frequency from 2-30 MHz.

These diode-laser systems[14] allow us to produce single-mode, narrow-band radiation that may be (1) tuned over 5 -10 GHz with several hundred hertz repetition rates, (2) stabilized to an atomic resonance with excellent long-term stability, or (3) frequency offset from a second laser with a digitally-controllable offset frequency in the range of 2-30 MHz. We have taken advantage of new, higher power diodes which have become available and we now have up to 35 mW available from some of these lasers. We now have ten grating-feedback laser systems working in our laboratory.

III. Rubidium atomic funnel

The atomic beam and atom interferometer are housed in a two-chamber, differentially pumped vacuum system. The source chamber is pumped with a turbomolecular pump and has a base pressure of 2×10^{-8} Torr and an operating pressure of 6×10^{-7} Torr when the rubidium oven is heated to produce the beam. The atomic funnel and interferometer are housed in a high vacuum chamber that is pumped with a trapped diffusion pump and has a base pressure of 3×10^{-9} Torr. The high vacuum chamber consists of a sphere with the funnel at its center and an adjacent cylinder for the atom interferometer. These two pieces were designed so that they can be attached in several different configurations with the pump on either chamber. This flexibility will be useful should we desire to try other possible interferometer configurations.

Figure 4 shows a schematic of the two-dimensional magneto-optic trap or atomic funnel. Zeeman slowing of a thermal atomic beam produces atoms that are loaded into the trap.[15,16] The thermal rubidium beam is produced by an effusive oven source with an aperture of 1 mm diameter. The oven is operated at a temperature of 235 °C and has a recirculation system to

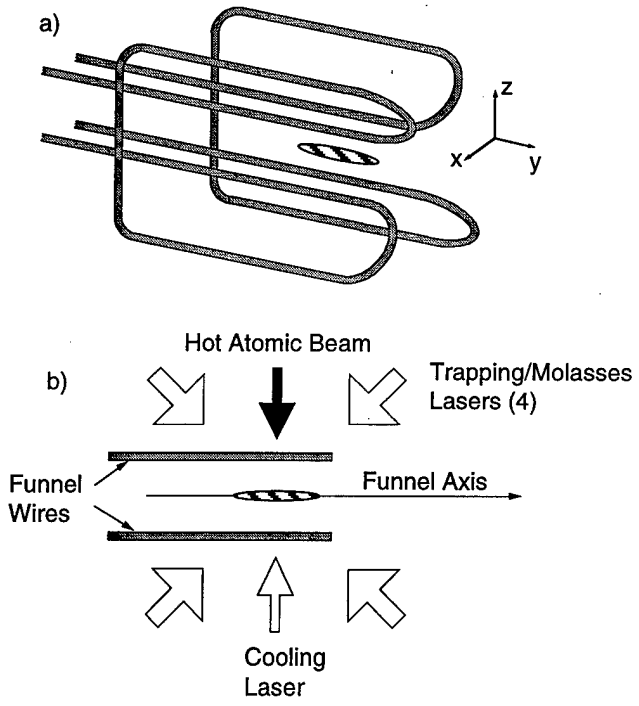

Fig. 4. (a) Funnel magnetic field wires in hairpin geometry. (b) Schematic of funnel showing lasers in horizontal (*xy*) plane. The origin of the coordinate system (shown displaced for clarity) is at the intersection of the funnel axis and the hot atomic beam. The cross-hatched area represents the region of trapping.

increase the time interval between oven reloadings.[17] The atomic beam propagates along the positive x-direction 1 m to the funnel region and is slowed and cooled by the scattering force from a counterpropagating laser beam tuned below the $F = 3$ to $F' = 4$ hyperfine transition of the D_2 line of ^{85}Rb. To compensate for the decreasing Doppler shift of the decelerating atoms, a spatially varying longitudinal magnetic field is imposed on the atoms. The field is designed so that the Zeeman shift changes in just the right manner to keep the atoms in resonance with a fixed laser frequency. We use σ^- polarized light to slow the atoms.[16] This method contrasts with standard σ^+ Zeeman cooling[15] in that the tapered magnetic field increases rather than decreases along the atomic beam. The 60-cm long magnet consists of a bias field of 360 G and a tapered field which approximates a field of

$$B_{taper} = 360\ \text{G} - 330\ \text{G}\sqrt{1 - \frac{z}{60\ \text{cm}}}\ . \qquad (1)$$

Figure 5 shows the Zeeman shift of the atoms resulting from the tapered and bias magnetic fields, which were measured with a Hall probe. Also shown are the Doppler shifts of atoms with different initial velocities and their evolution through the Zeeman slowing process. For the chosen detuning, we can slow atoms with initial velocities less than 250 m/s to a final velocity of 20 m/s. The dependence of the final velocity on the detuning of the laser frequency is shown in Fig. 6, along with the dependence for the case of σ^+ cooling (which can be achieved by subtracting rather than adding the bias and tapered fields). For final velocities below 100 m/s it is much easier to control the final velocity of the cooled beam in the case of σ^- cooling. This is an important feature for loading the atoms into a trap. A final velocity of approximately 20 m/s maximizes the number of atoms loaded into the trap; atoms with larger velocities cannot be trapped and atoms with smaller velocities tend to miss the trap due to their transverse velocity acquired during the one-dimensional slowing. With this Zeeman slower we typically have an order of magnitude more slow atoms than

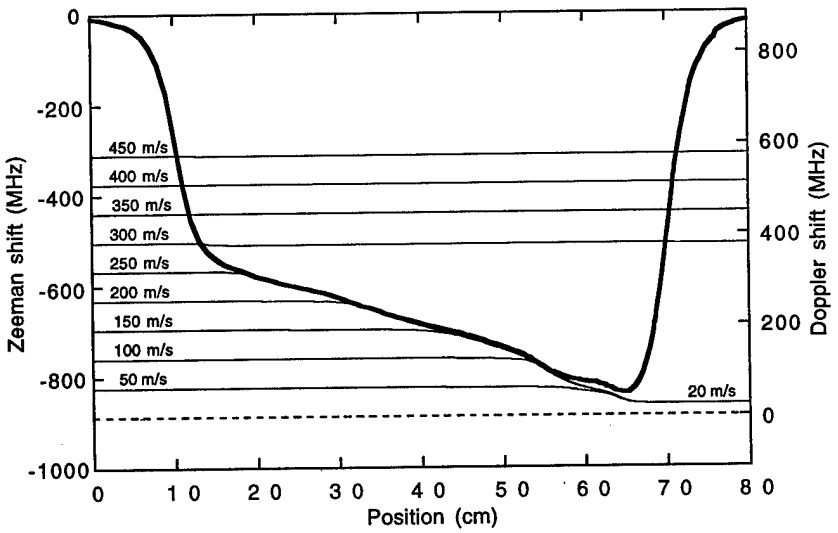

Fig. 5. Zeeman shift (bold line) and Doppler shift as a function of position in the tapered magnetic field. The Doppler shift curves are labeled with the initial atomic velocity and are results of an integration of the equation of motion. The two vertical axes have their origins offset by the laser frequency detuning (dashed line), so that the resonance condition is satisfied when the Zeeman shift and Doppler shift curves cross.

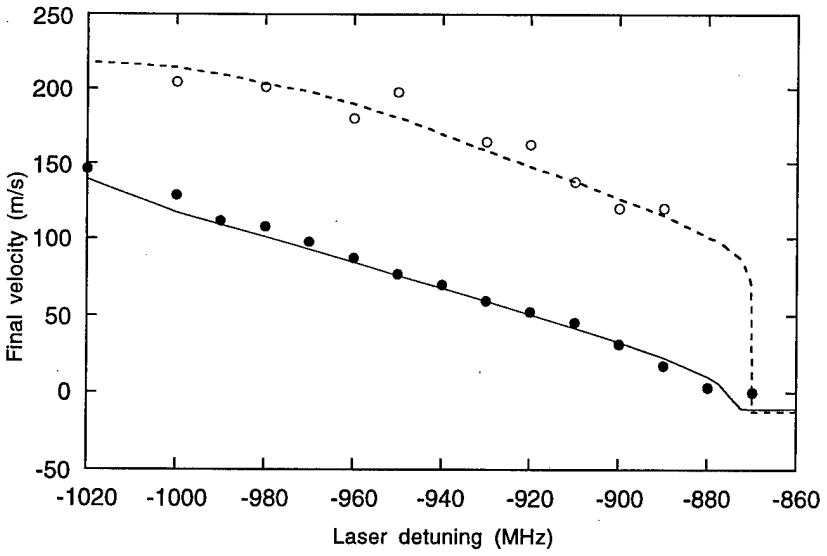

Fig. 6. Final velocity of slowed atoms as a function of laser frequency detuning. The solid line (dashed line) is from integration of the equation of motion of atoms moving through the Zeeman slower using σ^- (σ^+) cooling. The filled (open) circles are measurements for σ^- (σ^+) cooling (for the σ^+ data, the detuning has been offset to allow for easy comparison).

we did previously[5] using chirped cooling.[18] The main reason for this is that chirped cooling is inherently pulsed and hence has a duty cycle factor which reduces the efficiency.

The slow atoms drift into the two-dimensional magnetic quadrupole field in which six laser beams intersect to form the two-dimensional magneto-optic trap or atomic funnel. The atoms experience molasses-type damping[19] in all three dimensions and are trapped in the two dimensions transverse to the axis of the trap. The magnetic field of the funnel is formed by four parallel wires (copper tubing) arranged at the corners of a 2.5-cm-square, with alternating current directions. Each wire has a return path in a hairpin geometry,[6] as shown in Fig. 4. The return paths are located at the corners of a 6.3-cm-square and decrease the field by 20%. The wires carry a current of 70 A and are water cooled. The maximum field gradient is 13 G/cm in the *xz*-plane and decreases to 15% of this value 1 cm outside the end of the funnel.

The three orthogonal pairs of laser beams overlap at the intersection of the thermal beam and the funnel axis. The intensity in each beam is 8 mW/cm^2, or five times the saturation intensity. One counterpropagating σ^+-σ^- pair is along the z-axis, while the other two pairs are in the xy-plane and make angles of 45° with respect to the x- and y-axes. The beams along the z-axis are from a single laser at a frequency f. The beams with a propagation component along the positive y-axis come from a second laser tuned to a frequency $f + \Delta f$. The beams with a propagation component along the negative y-axis come from a third laser tuned to a frequency $f - \Delta f$. In the presence of the frequency shift Δf, atoms at rest will experience a force in the positive y-direction due to the imbalance in the scattering rates from the beams in the xy-plane. This moving molasses configuration[20] will result in a drift velocity $v = \sqrt{2}\lambda\Delta f$ (1.1 m/s/MHz for Rb) of the transversely trapped atoms. Atoms moving at the drift velocity see all six laser beams at the frequency f,[6] which permits the possibility of orientational cooling.[21] In contrast to the experiment of Riis *et al.*,[6] we have three-dimensional velocity compression without using a laser along the funnel axis, which allows unlimited downstream access to the beam. The other funnel experiments only used velocity compression in the two transverse directions.[7,8]

Fluorescence from atoms in the funnel is collected with a photomultiplier tube (PMT) and a CCD camera. The PMT signal indicates that approximately 10^9 - 10^{10} atoms/s are output from the funnel. The CCD image is used to optimize laser beam alignment in the funnel and to estimate the size of the atomic beam. To characterize the motion of the atoms, a standing-wave probe is placed downstream of the funnel. The probe beam is 1 mm wide (along the atomic beam direction) and 3 mm high and is placed 10 mm downstream from the end of the funnel. Fluorescence from this probe region is collected with a second PMT, and can also be viewed with a CCD camera. With red detuning, this standing-wave probe also provides one-dimensional transverse molasses damping of the atomic beam. Figures 7 and 8 show digitized video images of the funnel and downstream molasses region, viewed from the side and from the top, respectively. The side view (Fig. 7) shows the transverse spread of the beam as it travels downstream. That spread can be used to estimate a one-dimensional transverse temperature as discussed below. The

Fig. 7. Digitized video image of atoms in the atomic funnel. This side view shows the funnel at the left and the downstream probe region to the right. One of the wires (1/8" diameter) used to make the quadrupole magnetic field is visible near the top of the image.

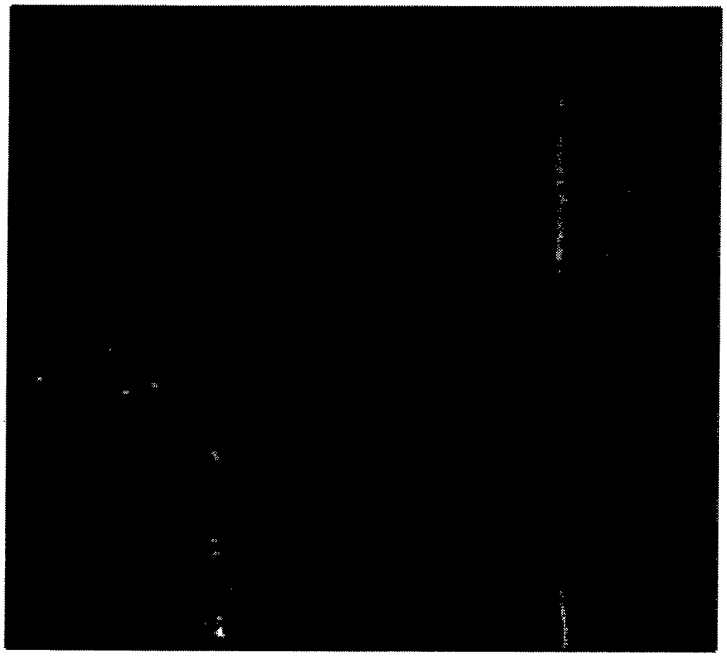

Fig. 8. Digitized video image of atoms in the atomic funnel. This top view shows the funnel at the bottom right and the downstream probe region at the upper right. One of the wires (1/8" diameter) used to make the quadrupole magnetic field is visible on the left side of the image.

other transverse dimension is seen in the top view (Fig. 8). In this dimension, the transverse molasses plays a role. There is still enough magnetic field gradient in this region to permit magneto-optic trapping to be effective, which explains why the downstream beam can be nearly the same size as the beam in the funnel.

To measure the velocity of the atomic beam, a time-of-flight technique is used.[6] Atoms near the exit end of the funnel are deflected using a resonant laser beam. The frequency of this laser is shifted off resonance for 2-3 ms to allow a short pulse of atoms to travel to the probe region. The transit time and spreading of this pulse as measured with the downstream probe fluorescence yield the mean beam velocity and the longitudinal temperature. The measured signals are fit to a function that models the funnel as a line of point sources, each with the same mean drift velocity and velocity spread.

A sample fluorescence signal and the resultant fit from the model are shown in Fig. 9. In this experiment, the pulse of atoms is long enough that the mean beam velocity is determined

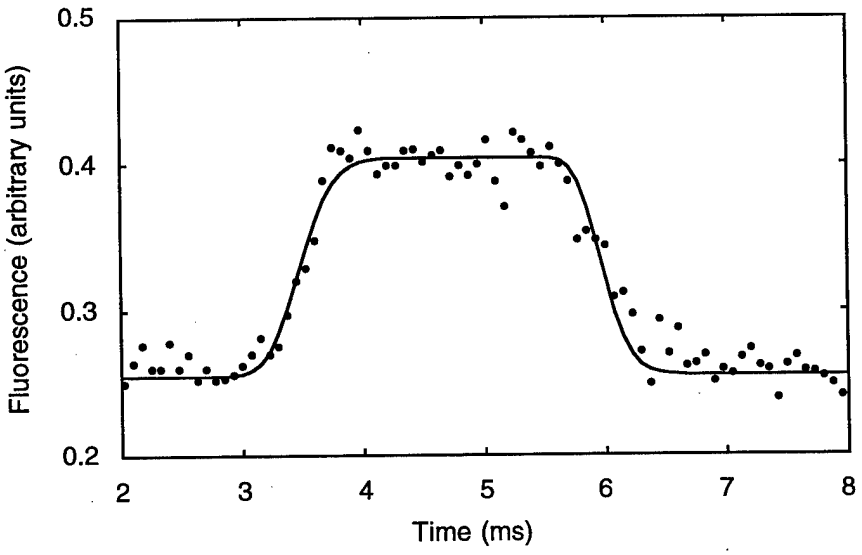

Fig. 9. Fluorescence signal from downstream probe laser used in time-of-flight analysis (filled circles). The solid line is a fit to the signal and yields the mean beam velocity and longitudinal temperature.

primarily by the delay of the leading edge of the pulse with respect to the gate and the longitudinal temperature is determined primarily by the slopes of the leading and trailing edges of the pulse. Data were taken for a range of values of the frequency offset Δf of the horizontal lasers from the vertical laser. Figure 10 shows the results of the measured beam velocity. The expected straight line $v = \sqrt{2}\lambda\Delta f$ is shown as a solid line. The data were taken with both our chirped cooling and Zeeman cooling configurations and so correspond to slightly different laser beam alignments and polarizations, and background magnetic fields. The data as a whole agree roughly with the expected moving molasses result. We have developed two models which might explain the discrepancies of the data from the expected result. The first model (shown as a dotted line in Fig. 10) accounts for laser beam misalignments, which can become important because the forces due to the counterpropagating laser beams in the trap can become unbalanced if the beams do not exactly overlap as the atoms leave the trap. We model this effect by simply letting the atoms leave the funnel with the expected velocity and then experience a short region of large acceleration.

The second model (shown as a dashed line in Fig. 10) assumes that the atoms experience an axial magnetic field caused by the earth's field and other magnetic equipment in the vicinity of

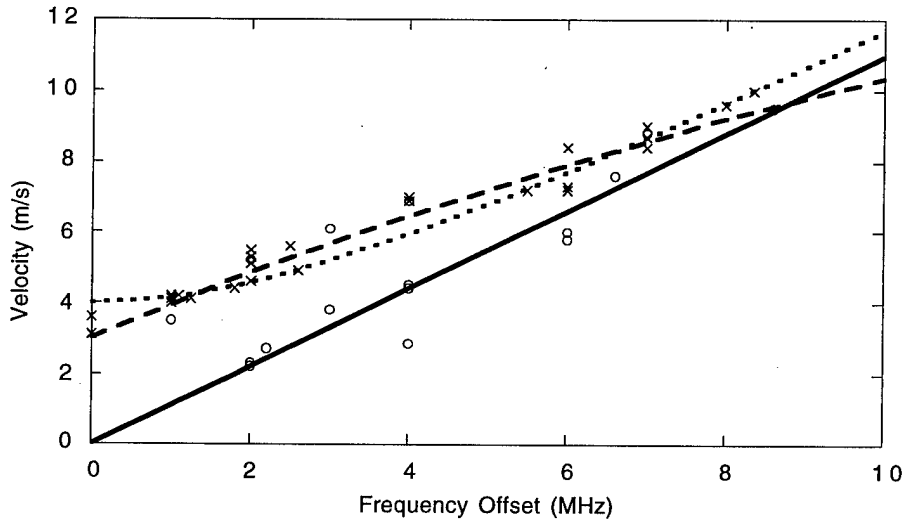

Fig. 10. Measured velocity of atoms leaving funnel as a function of the frequency offset Δf of the horizontal lasers. The open circles (crosses) correspond to data taken with Zeeman (chirped) cooling of the thermal beam. The solid line is the expected velocity of a moving molasses.

the vacuum chamber. A magnetic field B along the axis of σ^+-σ^- molasses leads to a drift velocity of the atoms of $v = -g_e \mu_B B / \hbar k$, where g_e is the excited state Lande factor, μ_B is the Bohr magneton, and k is the laser beam wavevector.[22] This effect would result in a change in the offset of the solid line shown in Fig. 10, but would not affect the slope. A change in slope can be explained by examining the dynamics of atoms as they enter and leave the trap. Atoms are damped to their final velocity with a characteristic time τ, which for simple one-dimensional Doppler cooling can be as short as 83 μs for rubidium, with a laser detuning of $\Gamma/2$. The damping time in our funnel is expected to be of order 1 ms, because of larger detunings used (2Γ and 3Γ) and deviations from an ideal two-level system. If the transit time of the atoms through the funnel is of the order of or less that the damping time, then the atoms will not have enough time to accelerate to the final expected velocity. The dashed curve in Fig. 10 shows the expected velocity for atoms that enter the funnel with no axial velocity and must travel 1 cm to leave the funnel. An assumed 4 G axial field is responsible for the non-zero velocity of atoms in the stationary molasses ($\Delta f = 0$), while an assumed damping time of 1.2 ms is responsible for the nonlinearity in the curve.

The time of flight signals yield a longitudinal temperature of $500\ ^{+500}_{-250}\ \mu K$. The transverse temperature is determined by CCD images of the atoms in the probe region. The expansion of the atoms at this point indicates a transverse temperature of $380\ ^{+80}_{-70}\ \mu K$. Both of these values are consistent with the Doppler cooling limit for rubidium of 300 μK (for a detuning of 2Γ), suggesting that orientational cooling is not present in our funnel.

To detect the atoms further downstream as well as behind the interferometer, we built a hot wire detector. A heated rhenium ribbon efficiently ionizes incident rubidium atoms and the ions are then multiplied by a pair of microchannel plates. With this detector we have been able to detect atoms up to 30 cm downstream of the funnel. The detector can be translated horizontally to measure the spatial profile of the cold atomic beam. Figure 11 shows the profile of the beam for a frequency offset of the horizontal trapping lasers of $\pm$ 7 MHz. The squares correspond to the measured detector signal with the background signal subtracted. The Gaussian curve was fit to the data assuming a 7.7 m/s longitudinal beam velocity. From the theoretical fit., the one-dimensional

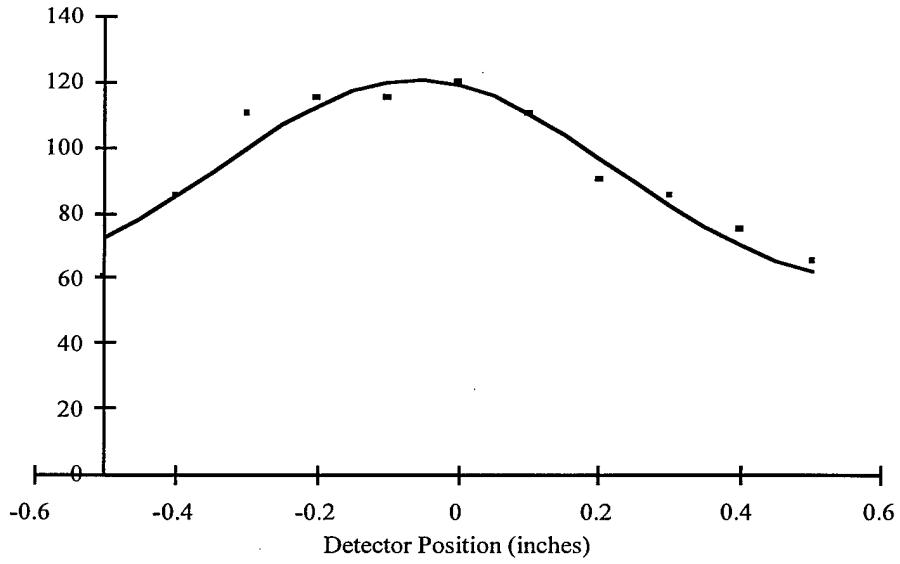

Figure 11. Spatial profile of the atomic beam 30 cm from the exit of the funnel for a horizontal trap laser detuning of ± 7 MHz. The squares correspond to the measured data. The solid line is the theoretical fit. For a velocity of 7.7 m/s, the calculated transverse beam temperature is $980\ ^{+130}_{-120}\ \mu K$.

horizontal transverse temperature of the beam was calculated to be $980^{+130}_{-120}\,\mu$K. This is consistent with what we measured in the probe region, assuming that the near-resonant standing-wave probe slightly heats the atomic beam that passes it.

IV. Grating fabrication

We have fabricated the amplitude transmission gratings to be used for the atom interferometer. We performed the work at the National Nanofabrication Facility (NNF) at Cornell University. The gratings were fabricated using the series of processing steps[9] shown in Fig. 12. A <100> oriented silicon wafer which is polished on both sides is first coated on both sides with 120 nm of silicon nitride using low pressure chemical vapor deposition (LPCVD). Free standing membranes or windows of the silicon nitride film are made by using optical lithography to pattern the back side of the wafer, reactive ion etching (RIE) in CF_4 to remove the patterned nitride, and a hot, wet etch in KOH to remove the exposed silicon. The wet KOH etches very slowly along the

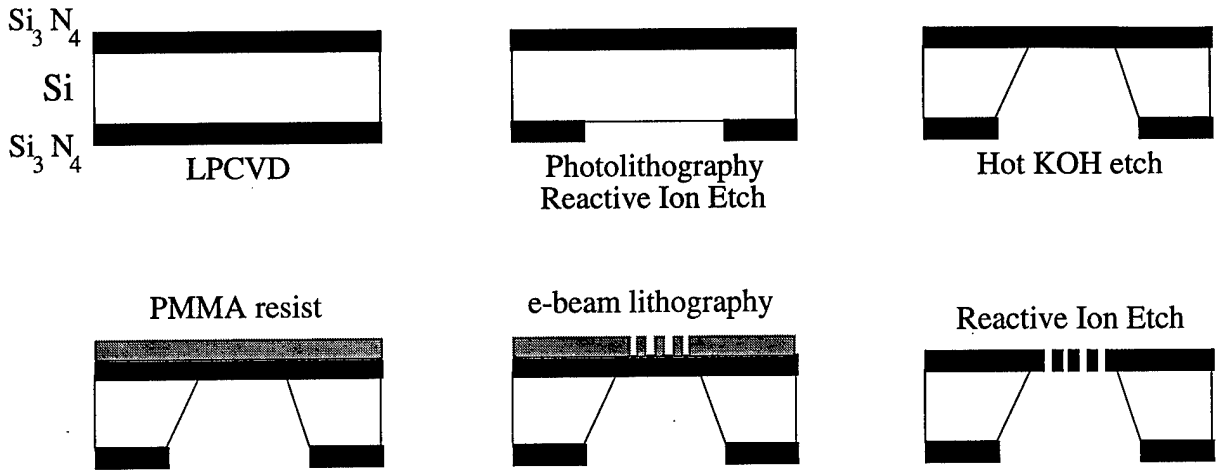

Fig. 12. Processing steps for grating fabrication.

<111> crystal planes, producing the beveled hole. The gratings are defined on these membranes using a JEOL JBX-5DII(U) electron-beam lithography system. Before exposure, the wafer is coated on the front side with 200 nm of polymethylmethacrylate (PMMA) and a thin ($\approx$ 20 nm) layer of gold to reduce writing distortions caused by substrate charging. The grating pattern is written in successive 80-μm "fields", with computer control to ensure that the fields are properly "stitched" together. After the grating is exposed, the PMMA is developed to leave a mask. The exposed silicon nitride is then removed using a reactive ion etch which was developed to be more selective and highly directional.[9] Figure 13 shows an SEM micrograph of part of a grating with a 250-nm grating spacing.

We have fabricated gratings with periods of 250 nm and 500 nm and with total areas of 1 mm x 150 μm, 1 mm x 50 μm, 0.5 mm x 150 μm, and 0.5 mm x 50 μm. Each 3" wafer is divided into 20 8 mm x 18 mm chips. Each chip has six atomic scale gratings, two larger optical scale gratings, and a marker window, as shown in Fig. 14. We were not as successful with the larger optical gratings (d = 8.4 μm) as with the atomic gratings. We designed the optical gratings for use in optical alignment of the interferometer and made the windows 1 mm x 1 mm in area, thinking that we could simply scale up the atomic gratings. However, the thickness of the nitride layer was obviously not scaled up, and this led to destruction of many of the optical gratings

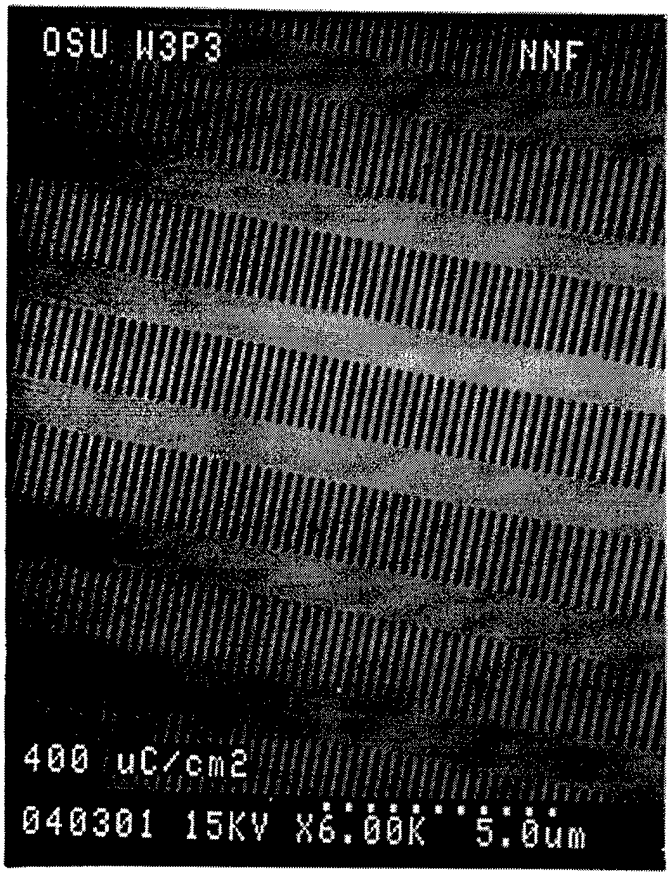

Fig. 13. SEM micrograph of a free-standing silicon nitride grating. The grating spacing is 250 nm and the spacing of the horizontal support bars is 4 μm.

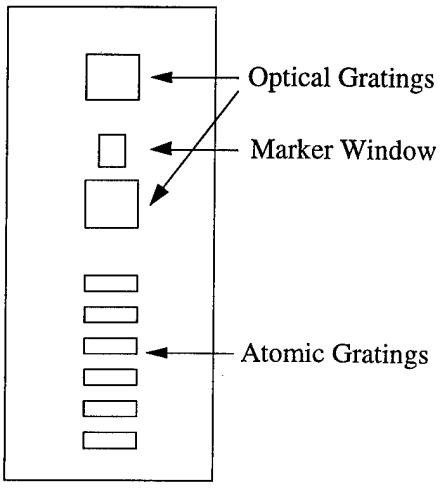

Fig. 14. Photolithographic pattern used to define free standing silicon nitride membranes.

during the last RIE step. We tried several methods and did meet with some success, though it was inconsistent.

To test the coherence of the atomic gratings we arranged for the electron-beam system to write verniers on the silicon substrate. By comparing verniers written in adjacent fields, we could determine the stitching errors. We found that the fields were correctly placed to within 10 nm between subsequent fields and to within 50 nm overall. Since this is a small fraction of the 250 nm grating spacing, the gratings are quite coherent.

V. Summary

In summary, we have produced a source of slow, cold rubidium atoms to be used as input to a three-grating atom interferometer for which we have also micro-fabricated silicon nitride gratings. This new interferometer will be a useful new tool in atomic physics, quantum optics, gravitation, and inertial sensing. In addition, the low velocities and high flux available from the funnel source will make this an attractive new source for other experiments in atom optics and atomic collisions.

VI. Personnel and publications

This research has been carried out with graduate students, undergraduate students, and a post-doctoral researcher. Three students have received the Ph.D. degree,[23-25] three students have received the M.S. degree,[26-28] and one undergraduate student did a senior thesis for the B.S. degree.[29]

Details of this research have been published in refereed journals[5,14,30] and have been presented at many national and international conferences.[31-37]

References

1 B. J. Chang, R. Alferness, and E. N. Leith, Appl. Opt. 14, 1592 (1975).

2 H. Mendlowitz and J. A. Simpson, J. Opt. Soc. Am. **52**, 520 (1962).

3 D. W. Keith, C. R. Ekstrom, Q. A. Turchette, and D. E. Pritchard, Phys. Rev. Lett. **66**, 2693 (1991).

4 E. L. Raab, M. Prentiss, A. Cable, S. Chu, and D. E. Pritchard, Phys. Rev. Lett. **59**, 2631-2634 (1987).

5 T. B. Swanson, N. J. Silva, S. K. Mayer, J. J. Maki, and D. H. McIntyre, J. Opt. Soc. Am. B **13**, 1833-1836 (1996).

6 E. Riis, D. S. Weiss, K. A. Moler, and S. Chu, Phys. Rev. Lett. **64**, 1658-1661 (1990).

[7] J. Nellessen, J. Werner, and W. Ertmer, Opt. Commun. **78**, 300-308 (1990).

[8] J. Yu, J. Djemaa, P. Nosbaum, and P. Pillet, Opt. Commun. **112**, 136-140 (1994).

[9] D. W. Keith, R. J. Soave, and M. J. Rooks, J. Vac. Sci. Technol. B **9**, 2846 (1991).

[10] B. Dahmani, L. Hollberg, and R. Drullinger, Opt. Lett. **12**, 876 (1987).

[11] A. Hemmerich, D. H. McIntyre, D. Schropp, Jr., D. Meschede, and T. W. Hänsch, Opt. Commun. **75**, 118 (1990).

[12] C. E. Wieman and L. Hollberg, Rev. Sci. Instrum. **62**, 1 (1991).

[13] C. Wieman and T. W. Hänsch, Phys. Rev. Lett. **36,** 1170 (1976).

[14] J. J. Maki, N. S. Campbell, C. M. Grande, R. P. Knorpp, and D. H. McIntyre, Opt. Commun. **102**, 251-256 (1993).

[15] W. D. Phillips and H. Metcalf, Phys. Rev. Lett. **48**, 596-599 (1982).

[16] T. E. Barrett, S. W. Dapore-Schwartz, M. D. Ray, and G. P. Lafyatis, Phys. Rev. Lett. **67**, 3483-3486 (1991).

[17] M. Lambropoulos and S. E. Moody, Rev. Sci. Instrum. **48**, 131-134 (1977).

[18] W. Ertmer, R. Blatt, J. L. Hall, and M. Zhu, Phys. Rev. Lett. **54**, 996-999 (1985).

[19] S. Chu, L. Hollberg, J. E. Bjorkholm, A. Cable, and A. Ashkin, Phys. Rev. Lett. **55**, 48-51 (1985).

[20] M. Kasevich, D. S. Weiss, E. Riis, K. Moler, S. Kasapi, and S. Chu, Phys. Rev. Lett. **66**, 2297-2300 (1991).

[21] J. Dalibard and C. Cohen-Tannoudji, J. Opt. Soc. Am. B **6**, 2023-2045 (1989); P. J. Ungar, D. S. Weiss, E. Riis, and S. Chu, J. Opt. Soc. Am. B **6**, 2058-2071 (1989).

[22] M. Walhout, J. Dalibard, S. L. Rolston, and W. D. Phillips, J. Opt. Soc. Am. B **9**, 1997 (1992).

[23] T. B. Swanson, Ph. D. Dissertation, "A Rubidium Atomic Funnel, " Oregon State University, 1995.

[24] N. J. Silva, Ph. D. Dissertation, "Laser Cooling and Trapping with Electronically Stabilized Grating-Feedback Diode Lasers, " Oregon State University, 1996.

[25] S. K. Mayer, Ph. D. Dissertation, " Low-velocity Matter-Wave Source for Atom Interferometry Produced by Zeeman-Tuned Laser Cooling and Magneto-Optic Trapping," Oregon State University, 1997.

[26] Holger Delfs, M.S. Dissertation, "A Magneto-Optic Trap for Rubidium," Oregon State University, 1992.

[27] Chris Cuneo, M.S. Dissertation, "Optically Stabilized Diode Laser using High-Contrast Saturated Absorption," Oregon State University, 1994.

[28] Peggy Lopez, M.S. Dissertation, "The Three-Grating Optical Interferometer used as a Monitoring and Stabilization Device for an Atomic Interferometer," Oregon State University, 1997.

[29] Kamand Mohamadzadeh, B. S. Senior Thesis, "Beam Isolation and Overlap Issues in the Three Grating Interferometer," 1992.

[30] C. J. Cuneo, J. J. Maki, and D. H. McIntyre, Appl. Phys. Lett. **64**, 2625-2627 (1994).

[31] A Rubidium Vapor Cell Trap: Applications to Atomic Interferometry (D. H. McIntyre, H. Delfs, and T. B. Swanson), **1992 Annual Meeting of the Division of Atomic, Molecular, and Optical Physics (DAMOP, APS)**, Chicago, Illinois, May 20-22, 1992. Bull. Am. Phys. Soc. **37**, 1139 (1992).

[32] Laser Cooling and Trapping of Rubidium: Applications to Atomic Interferometry (H. Delfs, T. B. Swanson, and D. H. McIntyre), **Book of Abstracts of the Thirteenth International Conference on Atomic Physics**, Munich, Germany, August 3-7, 1992, p. C10.

[33] Optically Stabilized Diode Laser using High-Contrast Saturated Absorption (C. J. Cuneo, J. J. Maki, and D. H. McIntyre), **1993 Interdisciplinary Laser Science Conference (ILS IX)**, Toronto, Canada, October 3-8, 1993; Bull. Am. Phys. Soc. **38**, 1714 (1993).

[34] Rubidium Atomic Funnel for Atom Interferometry (T. B. Swanson, J. J. Maki, N. S. Campbell, and D. H. McIntyre), **Technical Digest of the 1994 International Quantum Electronics Conference**, Anaheim, California, May 8-13, 1994, p. 37.

[35] A Rubidium Atomic Funnel (T. B. Swanson, J. J. Maki, N. S. Campbell, and D. H. McIntyre), **Book of Abstracts of the Fourteenth International Conference on Atomic Physics**, Boulder, Colorado, July 31- August 5, 1994, p. 1H-10.

[36] A Rubidium Atomic Funnel (N. J. Silva, T. B. Swanson, S. K. Mayer, J. J. Maki, and D. H. McIntyre), **Optical Society of America Annual Meeting**, Portland, Oregon, September 10-15, 1995.

[37] An Atomic Funnel for Atom Interferometry (D. H. McIntyre, S. K. Mayer, and N. J. Silva), **Atom Optics Conference, Photonics West '97**, San Jose, CA , February 8-14, 1997; published in **Atom Optics**, edited by M. G. Prentiss and W. D. Phillips, Proceedings of SPIE, **2995**, 68-77 (1997).